2023 IEEE/ASME International Conference on Advanced Intelligent Mechatronics (AIM)
June 28-30, 2023. Seattle, Washington, USA

Serial Chain Hinge Support for Soft, Robust and Effective Grasp

Dario Stuhne, Jelena Vuletić, Marsela Car and Matko Orsag

***Abstract*— This paper presents a serial chain hinge support, a rigid yet flexible structure that improves the mechanical performance and robustness of soft-fingered grippers. Gravity can reduce the integrity of soft fingers in horizontal approach, resulting in lower maximum payload caused by a large deflection of fingers. To substantiate our claim we performed multiple experiments on the payload and deflection of the SofIA gripper under both horizontal and vertical approaches. In addition, we show that this reinforcement does not impede the original compliant behavior of the gripper, maintaining the original kinematic model functionality. Also, we showcase the proprioceptive and exteroceptive capabilities for two opposing manipulation problems: grasping small and large objects. Finally, we validated the improved SofIA gripper in agricultural and everyday activities.**

I. INTRODUCTION

Driven by the ever-growing population and the accompanying food demand, impeded by climate change and labor shortage, traditional agriculture is rapidly changing [1]. Observing the latest rise of robotics and automation in agriculture, it is safe to pin them as key drivers of this change. In spite of this latest rise of robotics in agriculture, it has yet to reach the same level of success as in manufacturing industries. This is mostly because farming generally takes place in a very unstructured environment [2], be it in open fields or in greenhouses. However, in contrast to open fields, greenhouses offer a certain level of organization and structure, which can expedite the use of robots in everyday tasks such as harvesting, picking, pruning, pollination, etc. [3]. Harvesting crops is a perfect example of challenges in modern agriculture [1], mainly because it is time-consuming and labor-intensive. Picked fruits and vegetables can vary in size, mass, and shape (Fig. 1), which requires dexterity and adaptability that can be overcome by implementing soft robotics solutions [4]–[6], which are being intensively studied in agriculture for harvesting applications [7]–[9].

The quality of harvesting and, in a more general case, crop handling depends on how the soft gripper performs against gravity. To compare the performance of soft grippers against gravity authors in [1] group them into three categories (Fig. 2): (i) vertical approach from above, (ii) vertical approach from below, (iii) horizontal approach in the *x*-*y* plane (perpendicular to gravity). Only 15% of the grippers studied showed the ability to operate in both horizontal and vertical approaches. This drawback is particularly pronounced in soft two-finger grippers, since a smaller number of fingers in the gripper, together with the softness of the material, can only produce smaller payloads in the horizontal approach. When comparing payloads (sometimes referred to as gripping forces) of soft grippers for different approaches [10], [11], researchers report a significant decrease in the maximum payload for the horizontal approach compared to the vertical approach. In [12], 42% less payload was reported when using a soft gripper for versatile and delicate gripping in the horizontal approach, which has a significant negative impact on various agricultural tasks in that direction. Clearly, to mitigate the undesirable effects of gravity on the horizontal approach, additional reinforcements/improvements to the grippers are required.

The challenge this paper addresses is to eliminate the negative effects of gravity in the horizontal approach without impeding the working capabilities of the gripper in other directions (Fig. 2). The research follows up on our previous work [13] that presented a soft finger AI-enabled hand (SofIA,

Fig. 1: SofIA soft gripper mounted on FRANKA EMIKA Panda robotic arm handling fruit and vegetables (peppers, tomato, and strawberry) and miscellaneous everyday objects (a bottle, a coin, a paintbrush, scissors) in both horizontal and vertical approach. The serial chain hinge support is mounted on the outer side of the Fin-Ray finger structure.

*This work has been co-financed by Croatian Science Foundation under the project Specularia UIP-2017-05-4042. The work of doctoral student Jelena Vuletić has been supported in part by the “Young researchers’ career development project–training of doctoral students” of the Croatian Science Foundation funded by the European Union from the European Social Fund.

Authors are with LARICS Laboratory for Robotics and Intelligent Control Systems, University of Zagreb, Faculty of Electrical Engineering and Computing, Unska 3, 10000 Zagreb, Croatia `dario.stuhne, jelena.vuletic, marsela.polic, matko.orsag @fer.hr`

Fig. 1). Like other grippers reported in this paper SofIA's fingers deflect in a horizontal approach while producing larger payloads [13]. To solve this problem this study proposes using a serial chain hinge support. As we show in the paper, this improves SofIA's capabilities in the horizontal approach, at the same time ensuring that when the gripper is reinforced, its compliance and softness have not deteriorated. When it comes to handling delicate objects like picking ripe fruit, equally important as mechanical properties are the proprioceptive capabilities of soft grippers. Proprioception enables delicate closed-loop control during manipulation. In soft robotics it is often based on force and flex sensors [14], [15], but there have also been some efforts in the development of vision-based proprioceptive sensing [16], [17]. SofIA encompasses optical sensors, which enable real-time fingertip position tracking, supplementing a proposed gripper kinematic model. Additionally, the camera is positioned in a way that enables simultaneous finger posture and environment tracking, providing the possibility of exteroceptive sensing, which includes both grasp quality monitoring and target object detection and localization.

The main contribution of this paper is the novel serial chain hinge support that maximizes the payload, improves the mechanical properties of soft-fingered grippers in horizontal and vertical approach, and prevents the significant deflection of soft fingers. In addition to that, we show that the gripper kinematics has not deteriorated with the added hinge support and that the hinge support can be used to increase the sensory apparatus of the SofIA gripper. To test this hypothesis we conducted various experiments with objects of different shapes and sizes, reporting the results supporting our hypothesis in Section II. In Section III we demonstrate the mechanical properties and the perception capabilities in two opposing manipulation scenarios (i.e. manipulation of small and large objects). Putting it all together in Section IV, we show how serial chain hinge support does not impede the behavior of the ideal kinematic model of the Fin-Ray finger. Finally, we conclude the paper with examples of the variety of places in which SofIA has been benchmarked and validated such as RoboSoft 2022 competition and modern greenhouse.

II. Serial Chain Hinge Support

Hinges have recently attracted research attention in the development of soft grippers for different purposes. In [18], a shape memory alloy-based gripper with two hinge segments on each finger made from Ni-Cr wire was designed and developed. The main reason for using hinges was the controllability via two hinges, resulting in a total of nine different finger configurations for gripping [18]. Furthermore, a novel 3D-printed monolithic finger with built-in hinges for prosthetic applications was presented in [19]. In this monolithic finger design, the hinges were attached to the finger in the form of indentations, representing the location where the finger bends when actuated. However, this approach suffers from the fatigue of the finger material, since the finger loses elasticity and quenches after certain opening/closing cycles.

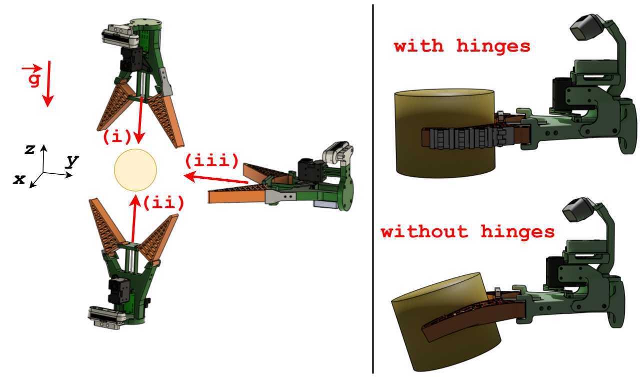

Fig. 2: **Left** - grasping approach directions with the respect to gravity. **Right** - the deflection in horizontal approach obtained from the point cloud for the gripper with and without the hinge support.

Compared to these existing attempts of integrating soft hinge-like structures, the study proposed in this paper is, to the best of our knowledge, the first attempt to utilize metal hinges as joints to reinforce the soft fingers without impeding soft capabilities. In this study hinges work as passive joints offering flexibility with their single degree of freedom (rotational joint between two plates). Ideally, hinges increase and improve the mechanical performance of SofIA's Fin-Ray fingers: the rigidity helps reduce the effects of deflection while spanning the range of maximum payload, with the initial softness and compliance of SofIA remaining intact due to the flexibility of joints connected in a serial chain.

This study builds upon our earlier work [13] where SofIA was originally presented as a soft gripper designed mainly for agricultural purposes. To facilitate handling objects of larger sizes and masses, while maintaining the same general principles and design elements presented in [13], we increased the size and modified the original Fin-Ray finger [20] with a longitudinal rib [13] to increase torsional stiffness. Additional modification to the soft body structure from this study introduces a cushion on the fingertip to enable the gripping of smaller objects (Fig. 3) which is discussed in Section IV in detail. The manufacturing procedure for the new fingers follows the same principles as presented in earlier work [13]. Soft fingers are made out of urethane rubber with a hardness of Shore 30A, and the actuation and mechanism type remained intact.

To reduce finger deflection, the serial chain hinge support must be attached to the body of the gripper. In this way, the shear forces and the bending moments that occur during grasping are taken over by the gripper's body, thus reducing the impact of deflection on the payload of the gripper. For this purpose, the serial chain is physically placed in the space between the lateral ribs on the outer side of the Fin-Ray finger structure, and the end of the chain is bolted to the side of the gripper's body. The serial chain hinge support consists of standardized steel door hinges and custom 3D-printed connectors. In choosing the standardized steel door hinge, we were constrained in terms of sizes that can be purchased.

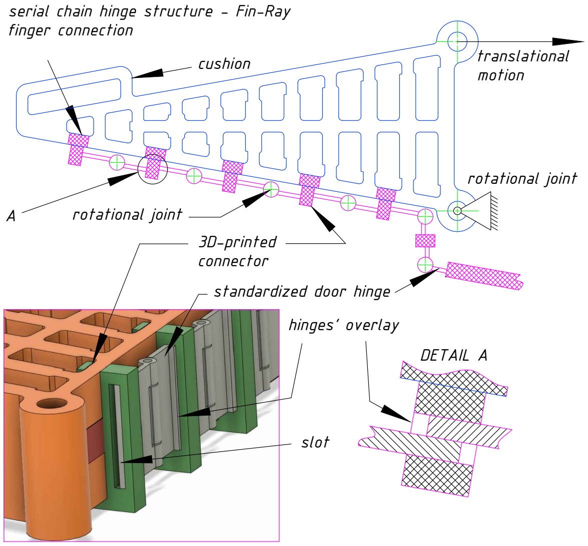

Fig. 3: Visualization of the implemented serial chain hinge support on the outer side of the Fin-Ray finger. The hinge support comprises 3D-printed connectors connecting standardized door hinges with a rotational joint. These connectors are attached to the Fin-Ray finger using a clip-on mechanism. The hinge support is bolted to SofIA's body, providing rigidity and flexibility to the fingers to minimize deflection, optimize mechanical performance without sacrificing softness and compliance.

However, we opted for the smallest one (20 mm in height) in order to make the serial chain compact and easy to integrate since the height of the Fin-Ray finger in SofIA is 22 mm. Furthermore, the role of 3D-printed connectors is two-fold. They serve: 1. to join the hinges allowing the two hinges to overlay within the same connector, 2. and to easily attach the serial chain to the outer side of the Fin-Ray finger (see Fig. 3). The hinge-to-hinge connection in these connectors cannot be rigid, i.e. bolted, bonded, etc. That is because the length of the outer side of the Fin-Ray finger (the side on which the serial chain is attached) expands and contracts during grasping. To support that, a linear degree of freedom should be allowed in every connector between two hinges. That offers the neighboring hinges to slide one against the other. This way the serial chain also expands and contracts along with the soft Fin-Ray structure. The dimensions of connectors are chosen based on: 1. the size of the hinges, 2. the overlay distance that needs to be allowed that hinges do not lose expanding and contracting functionality, and 3. the distance between two lateral ribs to allow easy attachment to the outer side of the Fin-Ray finger. The benefits of including serial chain hinge support to SofIA are explored and validated in detail. For this purpose, we subjected SofIA to payload and deflection studies. The payload and deflection studies were performed on the same setup that consists of SofIA soft gripper mounted on FRANKA EMIKA Panda robotic arm.

A. Payload

An extensive study on the effect of serial chain hinge support on SofIA payload is conducted in a series of experiments for which we used the setup visualized in Fig. 4. The first experiment investigates the payload capabilities depending on the grasped object size. We measured payload as a pull-out force as described in [21], i.e. the force that is reached at the moment when the object starts slipping from the grasp. A set of cylindrical primitives with varying diameters and approximately the same weight (less than 20 g) were used as payload objects in 4 experimental setups, namely for a gripper with hinge (*hinge*) and without hinge support (*basic*), and in both horizontal (HA) and vertical (VA) approaches. In each experiment, the same actuator input was given to the gripper to close its fingers always in the same position. The payload for each experiment was obtained as the average of four measurements for each object using a handheld weight scale. The maximum payload, i.e. the pull-

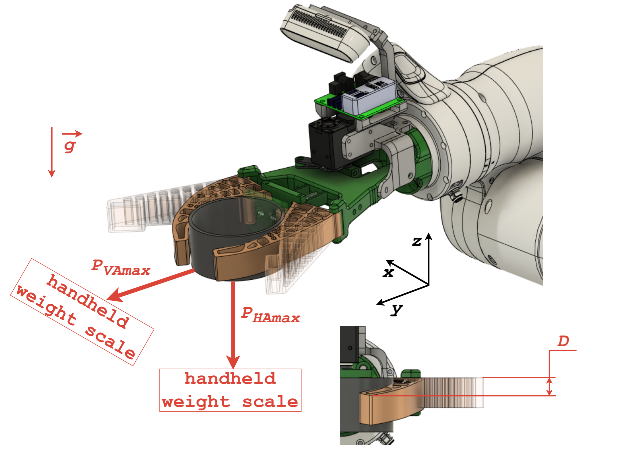

Fig. 4: Experimental setup for payload and deflection experiments. Payload was measured using a handheld weight scale in horizontal and vertical approaches. Results were determined visually. Deflection is calculated as the distance between two points before and after loading in the z-direction using Intel RealSense D435 depth camera data.

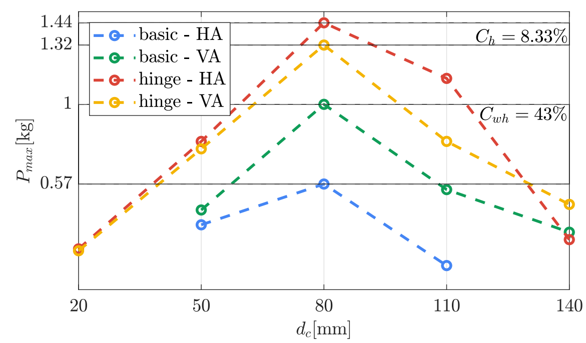

Fig. 5: Payload study for *basic* and *hinge* configuration in horizontal approach (HA) and vertical approach (VA). Moreover, the differences between the payloads for each configuration can be observed in the graph with a relative change of only 8.33% ($C_h = 8.33\%$) for the maximum payloads in HA and VA for *hinge* finger configuration compared to the relative change of 43% ($C_{wh} = 43\%$) for the maximum payloads in HA and VA for *basic* finger configuration.

out force was determined visually on the handheld weight scale. In the payload study, the payload could not be measured for three cases: a) *basic* - HA for $d_c = 20\,\text{mm}$, b) *basic* - HA for $d_c = 140\,\text{mm}$ and c) *basic* - VA for $d_c = 20\,\text{mm}$. In cases a) and c), the payload could not be measured for the *basic* configuration (without hinge support) in horizontal and vertical approaches for the smallest object in the experiments because of the twist of the fingers. The twist of the fingers can be defined as the fingers' state where fingers overlay during closing. On the contrary, the serial chain acts as a backbone to the fingers, keeping them in the same plane while bending, thus allowing that the payload can be measured. On the other side, in the case b) the payload could not be measured for the *basic* configuration in horizontal approach for the largest object in the experiments because that is the most vulnerable situation. As can be seen in Fig. 5, the *basic* finger configuration in horizontal configuration has overall the poorest results in terms of payload. In that manner, it is reasonable to conclude that the payload for object with 140 mm in diameter would be the smallest one in *basic* - HA compared to the other configurations. However, we could not measured the payload in this situation because it was smaller that the mass of the handheld weight scale (0.12 kg), which was the starting mass in the payload study.

Fig. 5 shows the identified relationship between the cylindrical objects diameter d_c and the maximum payload P_{max}. As expected the optimal performance is achieved for the medium-sized objects in accordance with other similar studies [21]. Deteriorated performance for smaller objects can be explained by lower contact forces between the object and the finger due to the smaller deformation of the finger. Due to the larger deformation of the finger, the overall mechanical performance deteriorates for larger objects when the actuator reaches its limits. The findings more relevant for this study are related to the comparison of maximum payloads for cases with and without hinges. Considering the *basic* SofIA configuration, we observe a higher maximum payload in vertical approach compared to the horizontal approach (43% higher). The deflection of the fingers increases together with the object's mass and size, which negatively affects mechanical performance in horizontal approach. The introduction of hinges improves the overall payload capabilities, increasing the maximum payload in both approach directions. An interesting finding of this study is the higher maximum payload in horizontal approach (8.33%), compared to vertical approach, for the SofIA gripper with hinges.

B. Deflection

The deflection, which is observed only in horizontal approach, is not completely eliminated by adding hinges to the side of the finger, but it is visibly smaller and less pronounced than without the hinge support (see Fig. 2). Fig. 6 shows the relationship between the payload P and the deflection D for each finger configuration. Payload study showed that both configurations (*basic* and *hinge*) exhibit optimal payload for an object with 80 mm in diameter (Fig. 5). Therefore, the

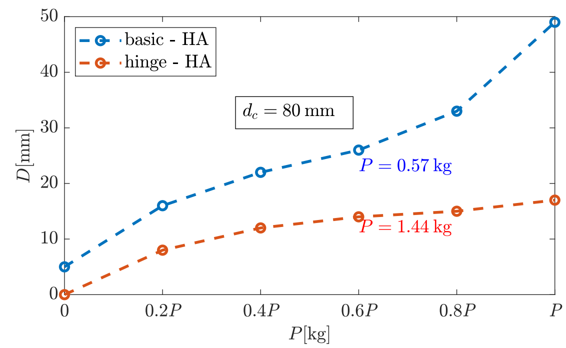

Fig. 6: Deflection study for *basic* and *hinge* configurations under different payloads P for both respective configurations in Fig. 5. Different payloads P were used in the study in order to relatively compare the deflection of both configurations (giving the best chance to each configuration in order to observe the worst-case scenario - the deflection under maximum payload for each configuration).

deflection experiment was conducted by gradually increasing the weight of the object with 80 mm in diameter to the weight that corresponds to the maximum payload P_{max} measured in HA for *basic* and *hinge* configuration. It is obvious that payloads for *basic* and *hinge* configurations differ, but the deflection is measured under different payloads to give the best chance to each configuration ($P_{basic} = 0.57$ kg and $P_{hinge} = 1.44$ kg). The same failure criterion was used for payload and deflection experiments, i.e. when the object starts to slip from the grip. The results in Fig. 6 clearly show that the deflection is significantly smaller for the *hinge* configuration, which confirmed our initial hypothesis in adding hinges to the gripper.

During each sequence of the deflection experiment, the point cloud was recorded from the Intel Realsense D435 depth camera that is a part of the SofIA's sensory system (described in Section III). Then, we calculated the deflection as the distance between the same point (fingertip) in two different conditions (1. unloaded state, 2. loaded state) in z-direction (see Fig. 3).

III. Perception

SofIA's sensory system consists of an RGB-D camera, Intel RealSense D435, mounted so that both exteroception (environment sensing) and proprioception (grasp quality assessment and kinematic behaviour monitoring) are available simultaneously. Proprioception has been used both for validation of the kinematic model, enabling accurate comparison of finger behaviour for *basic* and *hinge* configuration, and as a supplement for the kinematic model, which is further discussed in Section IV.

On the other hand, SofIA's exteroceptive capabilities are crucial for planning, as executing a stable grasp of objects of different sizes requires estimation of the size of an object which is to be grasped. Additionally, SofIA's choice between the two possible approach directions (horizontal and vertical) depends on the target object's dimensions. In our previous

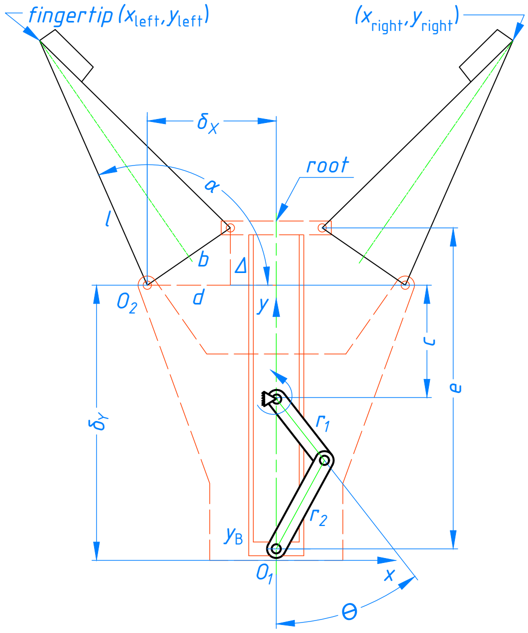

Fig. 7: Geometric relationships between the main features of SofIA used to derive the kinematic model. During the actuation of the motor, the position of the slider Δ changes, resulting in the rotation of the fingertip around the point O_2. Knowing the exact mathematical expression of the change in the fingertip position with respect to the change in DC motor rotation angle θ enables the better planning of grasping of both larger and smaller objects.

work [22], we used a convolutional neural network to detect and harvest peppers by extracting grasping target dimensions from the depth image recorded with an RGB-D camera. This approach worked well for agricultural applications and fruit picking. The same approach was simplified for the RoboSoft 2022 competition which was another opportunity to benchmark the gripper. In all of the tasks, various objects that had to be detected autonomously were placed on a flat surface in front of the robotic arm. First, we recorded point clouds from multiple angles, transformed them from the camera frame to the global coordinate frame, and registered the transformed point clouds. The registered point cloud was then filtered based on *a priori* known information about the environment, i.e. the bounding boxes in which objects could be placed. The remaining filtered points were used to estimate the object dimensions and to decide on the grasping approach based on the most dominant object dimension, taking into consideration the kinematic limitations of the robotic arm.

IV. Modeling and Grasping

A. Kinematic Model

The results presented in Sections II-A and II-B allow us to conclude that serial chain significantly improves the mechanical properties of the gripper in terms of maximizing the payload and reducing the deflection. Still, the serial chain is a stiff structure. Thus, our goal is to find out in which amount serial chain affects opening/closing of the fingers. Therefore, this Section deals with ideal kinematic model of SofIA. When in unloaded state (not in contact with the object), the Fin-Ray finger can be modeled as rigid body which is taken as an assumption in creating the kinematic model. By adding serial chain to the Fin-Ray finger, the same behavior is kept.

Slider-crank linkage, driven by a DC servomotor, is a core mechanism that enables finger movement in the SofIA gripper. It converts rotational motion into translational, moving the position of y_B along the y-axis (Fig. 7):

$$y_B = r_1 \cdot \cos(\theta) + \sqrt{r_2^2 - r_1^2 \cdot \sin^2(\theta)}, \tag{1}$$

where θ stands for the input motor angle and r_1 and r_2 denote the length of the crank and the rod connecting the crank and the slider, respectively. Controlling the position of y_B moves the slider position Δ and shapes the finger base length b:

$$\Delta = e - c - y_B \tag{2}$$

$$b = \sqrt{d^2 + \Delta^2}. \tag{3}$$

The fingers are modeled as isosceles triangles with constant leg length l and variable base angle and base length b. The change in the base angle of the soft finger is taken into account when calculating the fingertip angle of rotation α around the point O_2:

$$\alpha = \arcsin(\frac{\Delta}{b}) + \arccos(\frac{b}{2l}). \tag{4}$$

Finally, the positions of both the left and the right finger are calculated as follows:

$$x_{left} = l \cdot \cos(\alpha) - \delta_x \tag{5}$$

$$x_{right} = \delta_x - l \cdot \cos(\alpha) \tag{6}$$

$$y_{left} = y_{right} = l \cdot \sin(\alpha) + \delta_y, \tag{7}$$

where δ_x and δ_y denote distances from O_2 to the center of SofIA coordinate system O_1.

In order to compare the ideal model with the actual behavior of both the *hinge* and the *basic* version of SofIA, fingertip position was recorded using SofIA's proprioceptive capabilities. Fingertips were marked with red pins and thus straightforwardly filtered in HSV color space in the image recorded with Intel RealSense D435 camera. SofIA was repeatedly opened and closed in increments of 0.015 rad. Position of the fingertip was extracted in the image for each increment, and its 3D position in the camera coordinate frame was obtained using the corresponding registered point cloud. Finally, as the camera was calibrated using the procedure described in [23], the transformation from the SofIA coordinate frame to the camera coordinate frame $\mathbf{T}_S^C$ was known *a priori* and used to transform the fingertip position from the camera coordinate frame to the SofIA coordinate frame. Fingertip positions in both opening and closing sequences, along with the dissipation across 10 experiment repetitions, for both SofIA configurations are shown in Fig. 8. Maximum and minimum motor angles on Fig. 8 correspond to the fully open (-0.8 rad) and the fully closed (-1.4 rad) gripper positions, respectively.

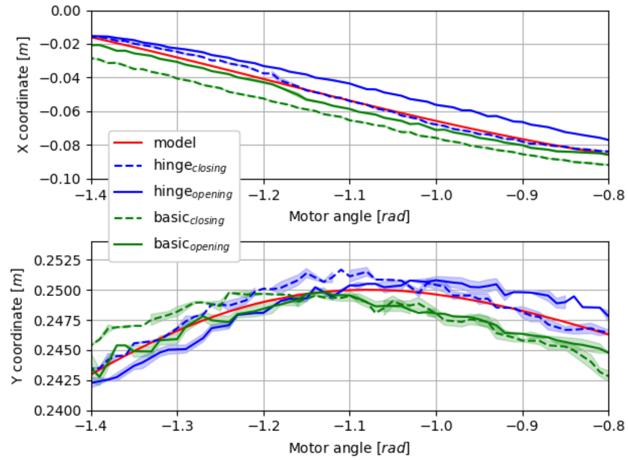

Fig. 8: SofIA kinematics shown for the left finger for *basic* and *hinge* finger configuration, compared to the proposed kinematic model. The position of the fingertip was recorded in 10 experiment repetitions for both structures, where a single repetition consisted of both opening and closing the SofIA.

As can be seen in Fig. 8, SofIA gripper reinforced with the proposed hinge support follows the derived ideal kinematic model more precisely than the original not reinforced version. While the deviation from the model on Y coordinate is on a millimeter scale for both structures, differences along X axis reach up to 1 cm in opposite directions for different structures. On one hand, the hinges tend to prevent the gripper from reaching the fully open position, resulting in lower X coordinate values for the left fingertip position, while on the other hand, the finger without the supporting structure exceeds the modeled maximum gripper opening. The deviation between the closing and the opening sequence is also observed in both cases and is a consequence of backlash in mechanism.

B. Grasp Planning Strategy

Considering that both the finger length (Y coordinate in Fig. 8, i.e. the tip of the grasp) and the slider position Δ (Eq. 2, i.e. the root of the grasp) vary as a function of the joint, grasping objects of different sizes requires different approaches. Two edge cases, namely grasping of large ($\geq$ 80 mm in diameter) and small ($\leq$ 10 mm height) objects, have been examined as a part of this study, demonstrating improvement introduced with the serial chain hinge support, while retaining compliant properties of the original version of SofIA. A stable grasp of bigger objects has to be enveloping, i.e. the entire volume of the target object has be contained between the fingers. In order to achieve that, the motion of the root of the grasp Δ has to be compensated with the robotic arm motion t. The SofIA's mounting point must move in the opposite direction along the same axis while closing the gripper (Fig. 9). That way, the grasped object will be positioned as close to the gripper body as possible, ensuring maximum grasp stability. For small objects, a successful grasp can be achieved thanks to the cushions attached to the fingertips (Fig. 3). However, when

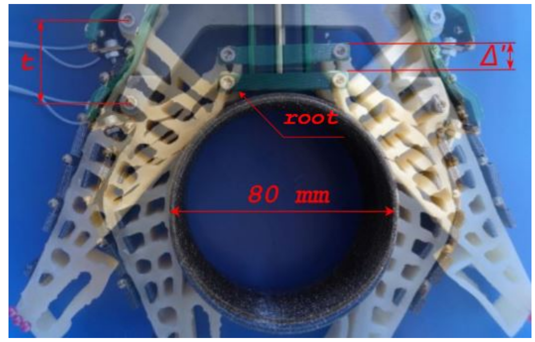

Fig. 9: Overlay of fully open SofIA before the grasp and fully closed SofIA grasping the target object. Robotic arm translated along the grasping axis for t in order to compensate for total slider displacement Δ. Slider displacement Δ' remained uncompensated.

grasping small objects, it has to be ensured that the grasped object is positioned between the centers of the cushions once the gripper is fully closed. As the position of the fingertips on y-axis decreases when closing the gripper, the robotic arm has to compensate for the displacement of the fingertips, which can easily be achieved if the proposed kinematic model is taken into account when planning the grasp, since we show that hinge finger configuration follows the proposed kinematic model satisfyingly.

A special case of small object grasping occurs when objects small in height are placed on a flat surface, which was one of the tasks in RoboSoft 2022 competition and is common in many other manipulation tasks such as small parts assembly. Such objects have to be approached in the vertical direction in order to avoid collision of the robotic arm with the flat surface during manipulation. In the proposed scenario, in order for grasp to be successful, the fingertip position in y-axis in SofIA coordinate frame calculated using the proposed kinematic model would be larger ($> y_S$) than the y-axis coordinate of the flat surface $y_S = 0.235$ (Fig. 10), detected in the same coordinate frame. Passive compliance of SofIA fingers enables the successful execution of small object grasping task by sliding along the surface while approaching the grasping pose. The position of the fingertip in sliding mode is shown in Fig. 10. During the whole grasping procedure, the fingertip position in y-axis is approximately constant and corresponds to y_S. The small deviations of the fingertip position in y-axis from the y_S can be attributed to the measurement errors and finger thickness. It can also be seen that the gripper does not fully close at -1.4 rad, which is the modeled behaviour in the contactless scenario, but it instead reaches a fully closed position at -1.9 rad. At this point, the object is successfully grasped and the upper part of the finger is no longer bent. The bending can be observed as the difference between the no-contact model and sliding response in Fig. 10.

V. Conclusion

The SofIA gripper, specifically designed for agricultural applications, was successfully validated on various tasks such as picking peppers, strawberries, tomatoes, holding flowers for

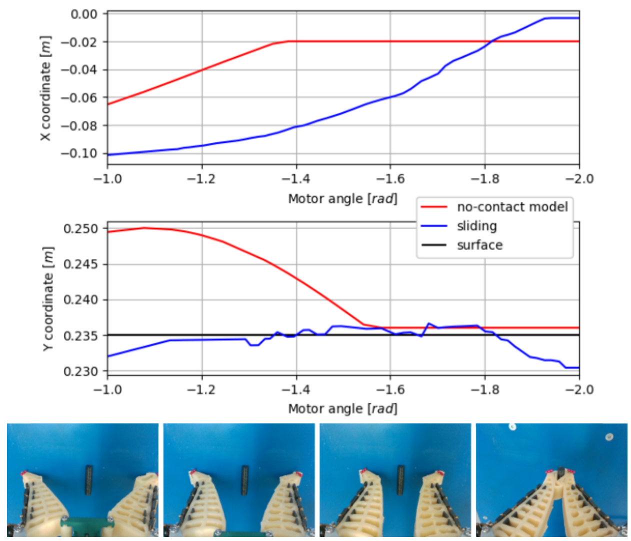

Fig. 10: Position of the left fingertip for the *hinge* finger configuration SofIA in a sliding mode, position obtained from the kinematic model and position of a flat surface on which an object is placed. Due to compliant nature of SofIA, fingers slide along the surface, which enables successful grasp of a small object placed on the flat surface. The positions of the fingertip and the surface are shown in SofIA coordinate system O_1 (Fig. 7). Finger positions recorded during the grasping procedure are shown under the graph.

pollination, and delicate strawberry picking. It demonstrated effectiveness even with heavier tomatoes by utilizing the support of hinges. To further assess the capabilities of the serial chain hinge support, SofIA was tested in three scenarios of the 2022 RoboSoft competition: pick and place task, potted plant transportation, and pouring from a bottle and serving. These tasks aimed to showcase the gripper's softness, robustness, and effectiveness in everyday activities. All tasks were completed successfully, as shown in the supplemental and YouTube videos [24]. The addition of the serial chain hinge support significantly enhanced the mechanical performance and robustness of SofIA, enabling it to handle larger payloads (32% more in the vertical approach and 252% more in the horizontal approach). It also reduced the relative changes between payloads in horizontal and vertical approaches (43% relative change for *basic* finger configuration and only 8.33% for *hinge* finger configuration), as well as the deflection gradient in the horizontal approach. The hinge support had minimal impact on the kinematics of the *basic* SofIA configuration. Furthermore, the improved mechanical capabilities, kinematic model, and proprioceptive features of the gripper allowed it to excel in grasping both small and large objects.

REFERENCES

[1] J. F. Elfferich, D. Dodou, and C. D. Santina, "Soft robotic grippers for crop handling or harvesting: A review," *IEEE Access*, vol. 10, pp. 75428–75443, 2022.

[2] B. Zhang, Y. Xie, J. Zhou, K. Wang, and Z. Zhang, "State-of-the-art robotic grippers, grasping and control strategies, as well as their applications in agricultural robots: A review," *Computers and Electronics in Agriculture*, vol. 177, 2020.

[3] M. Polic, A. Ivanovic, B. Maric, B. Arbanas, J. Tabak, and M. Orsag, "Structured ecological cultivation with autonomous robots in indoor agriculture," in *2021 16th International Conference on Telecommunications (ConTEL)*, pp. 189–195, 2021.

[4] C. Tawk, A. Gillett, M. I. H. Panhuis, G. M. Spinks, and G. Alici, "A 3d-printed omni-purpose soft gripper," *IEEE Transactions on Robotics*, vol. 35, 2019.

[5] M. Manti, T. Hassan, G. Passetti, N. D'Elia, C. Laschi, and M. Cianchetti, "A bioinspired soft robotic gripper for adaptable and effective grasping," *Soft Robotics*, vol. 2, 2015.

[6] S. Abondance, C. B. Teeple, and R. J. Wood, "A dexterous soft robotic hand for delicate in-hand manipulation," *IEEE Robotics and Automation Letters*, vol. 5, 2020.

[7] E. Navas, R. Fernandez, D. Sepulveda, M. Armada, and P. Gonzalez-De-Santos, "Soft gripper for robotic harvesting in precision agriculture applications," *2021 IEEE International Conference on Autonomous Robot Systems and Competitions, ICARSC 2021*, 2021.

[8] E. Navas, R. Fernández, D. Sepúlveda, M. Armada, and P. Gonzalez-De-santos, "Soft grippers for automatic crop harvesting: A review," *Sensors*, vol. 21, 2021.

[9] A. Gunderman, J. Collins, A. Myers, R. Threlfall, and Y. Chen, "Tendon-driven soft robotic gripper for blackberry harvesting," *IEEE Robotics and Automation Letters*, vol. 7, pp. 2652–2659, 4 2022.

[10] J. Zhou, X. Chen, J. Li, Y. Tian, and Z. Wang, "A soft robotic approach to robust and dexterous grasping," *2018 IEEE International Conference on Soft Robotics, RoboSoft 2018*, 2018.

[11] G. B. Crowley, X. Zeng, and H. J. Su, "A 3d printed soft robotic gripper with a variable stiffness enabled by a novel positive pressure layer jamming technology," *IEEE Robotics and Automation Letters*, vol. 7, 2022.

[12] A. T. Mathew, I. Hussain, C. Stefanini, I. M. B. Hmida, and F. Renda, "Resoft gripper: A reconfigurable soft gripper with monolithic fingers and differential mechanism for versatile and delicate grasping," *2021 IEEE 4th International Conference on Soft Robotics, RoboSoft 2021*, 2021.

[13] D. Stuhne, J. Tabak, M. Polić, and M. Orsag, "Design and prototyping of soft finger ai-enabled hand (sofia)," in *2022 IEEE/ASME International Conference on Advanced Intelligent Mechatronics (AIM)*, pp. 1581–1586, 2022.

[14] H. Wang, M. Totaro, and L. Beccai, "Toward perceptive soft robots: Progress and challenges," *Advanced Science*, vol. 5, p. 1800541, 07 2018.

[15] B. S. Homberg, R. K. Katzschmann, M. R. Dogar, and D. Rus, "Robust proprioceptive grasping with a soft robot hand," *Autonomous Robots*, vol. 43, 2019.

[16] M. Polic, I. Krajacic, N. Lepora, and M. Orsag, "Convolutional autoencoder for feature extraction in tactile sensing," *IEEE Robotics and Automation Letters*, vol. 4, no. 4, pp. 3671–3678, 2019.

[17] F. Hundhausen, J. Starke, and T. Asfour, "A soft humanoid hand with in-finger visual perception," pp. 8722–8728, 10 2020.

[18] W. Wang and S. H. Ahn, "Shape memory alloy-based soft gripper with variable stiffness for compliant and effective grasping," *Soft Robotics*, vol. 4, 2017.

[19] R. Mutlu, G. Alici, M. I. het Panhuis, and G. M. Spinks, "3d printed flexure hinges for soft monolithic prosthetic fingers," *Soft Robotics*, vol. 3, 2016.

[20] Festo.com, "Adaptive gripper finger dhas." `https://www.festo.com/cat/en-gb_gb/data/doc_ENGB/PDF/EN/DHAS_EN.PDF`, 2022.

[21] Y. Sun, Y. Liu, F. Pancheri, and T. C. Lueth, "Larg: A lightweight robotic gripper with 3-d topology optimized adaptive fingers," *IEEE/ASME Transactions on Mechatronics*, vol. 27, no. 4, pp. 2026–2034, 2022.

[22] M. Polic, J. Tabak, and M. Orsag, "Pepper to fall: a perception method for sweet pepper robotic harvesting," *Intelligent Service Robotics*, 2021.

[23] B. Maric, M. Polic, T. Tabak, and M. Orsag, "Unsupervised optimization approach to in situ calibration of collaborative human-robot interaction tools," in *2020 IEEE International Conference on Multisensor Fusion and Integration for Intelligent Systems (MFI)*, pp. 255–262, IEEE, 2020.

[24] LaricsLab, "Serial chain hinge support for sofia." `https://www.youtube.com/playlist?list=PLC0C6uwoEQ8YZfoCRMe0X0HLZsRzIMQCY`, 2022.